Chapter 9
Photovoltaic System: Case Studies

Ali Durusu, Ismail Nakir and Mugdesem Tanrioven

Abstract Solar energy is one of the most important energy, which is environmentally friendly such as clean, inexhaustible and free, among the renewable energy sources. Studies on solar photovoltaic (PV) energy generation system were promoted in last two decades. The main application of PV systems are in stand-alone (water pumping, lighting, electrical vehicle, etc.), hybrid and grid-connected (PV power plants) configuration. Stand-alone PV power generation system is considered as good alternative for places that are far from conventional power generation/transmission/distribution system. PV generation systems have two big problems; PV conversion efficiency is very low and PV electricity generation is effected from changing of weather condition. PV output varies periodically in a year and in a day, and is not stable due to environmental condition. Accordingly, in order to increase PV output and PV efficiency, it is crucial to analyze PV output considering solar radiation, temperature, wind speed, shadow, etc. Maximum power point trackers (MPPTs) are employed for extracting power from photovoltaic (PV) panels. MPPTs enforce the solar modules to operate at maximum power point (MPP) under the fluctuations of ambient conditions. Therefore, they take a vital role for increasing of PV system efficiency. In this part, the case studies of MPPT system, which includes stand-alone and hybrid PV systems, will be briefly reviewed, followed by discussion of the MPPT modeling, design, etc. Several stand-alone and hybrid MPPT application will be presented. Latest developments in MPPT methods will be summarized. Finally some of the present challenges facing the MPPT techniques will be explored.

Keywords Photovoltaic systems · Case studies · MPPT algorithms · MPPT algorithm modeling

A. Durusu (✉) · I. Nakir · M. Tanrioven
Yildiz Technical University, Davutpasa Campus, 34220 Istanbul, Turkey
e-mail: adurusu@yildiz.edu.tr

I. Nakir
e-mail: inakir@yildiz.edu.tr

M. Tanrioven
e-mail: mtanrioven@gmail.com

N. Bizon et al. (eds.), *Energy Harvesting and Energy Efficiency*,
Lecture Notes in Energy 37, DOI 10.1007/978-3-319-49875-1_9

Abbreviation and Acronyms

IC	Incremental Conductance
MPP	Maximum Power Point
MPPT	Maximum Power Point Tracker
OC	Only Current Photovoltaic
P&O	Perturbation and Observe
PV	Photovoltaic
SC	Short Circuit Current
THD	Total Harmonic Distortion

9.1 Introduction

Solar energy is one of the most important energy, which is environmentally friendly such as clean, inexhaustible and free, among the renewable energy sources [1]. Studies on solar photovoltaic (PV) energy generation system were promoted in last two decades. The main application of PV systems are in stand-alone (water pumping, lighting, electrical vehicle, etc.), hybrid and grid-connected (PV power plants) configuration. Stand-alone PV power generation system is considered as good alternative for places that are far from conventional power generation/transmission/distribution system. Such systems applications presented in two scale: application at a small scale from 1 to 10 kW and stand-alone PV system in size, from 10 to 100 kW [2]. In hybrid PV systems, more than one type of electricity generator, such as wind turbine, fuel cell, diesel generator, etc., is employed. In grid-connected PV systems, it is usual practice to connect PV system to the electricity grid [3]. A grid-connected PV system provides parallel work with the already established electricity grid and number of PV system features are determined by this connection to the utility grid [4]. PV capacity in the world, including stand-alone, hybrid and grid connected, is rapidly increasing. Figure 9.1 shows the global PV total capacity from 2004 to 2014.

It is clear from the Fig. 9.1 that, 40 GW capacity added in 2014 and also more than 60% of all PV capacity in operation worldwide at the end of 2014 was added over the past 3 years [5].

PV generation systems have two big problems; PV conversion efficiency is very low and PV electricity generation is effected from changing of weather condition [6]. PV output varies periodically in a year and in a day, and is not stable due to environmental condition. Accordingly, in order to increase PV output and PV efficiency, it is crucial to analyze PV output considering solar radiation, temperature, wind speed, shadow, etc.

Maximum power point trackers (MPPTs) are employed for extracting power from photovoltaic (PV) panels. MPPTs enforce the solar modules to operate at MPP under the fluctuations of ambient conditions. Therefore, they take a vital role for

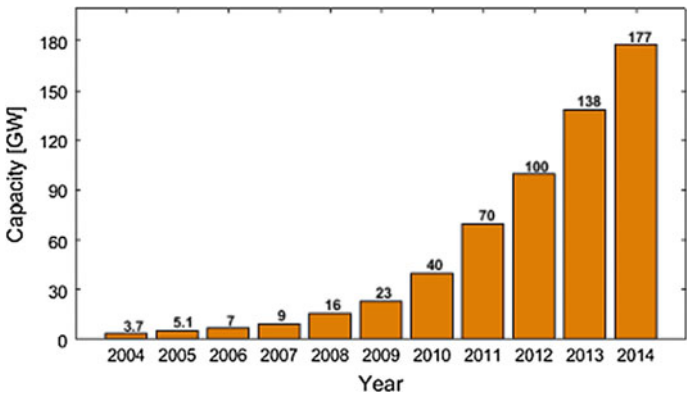

Fig. 9.1 PV total installed capacity from 2004 to 2014 in the world [5]

increasing of PV system efficiency. Different MPPT algorithms are used for the determination of MPP. These algorithms are divided into two groups: direct and indirect. In indirect algorithms, the operating point, where PV generator operates with maximum power, is estimated either measuring current, voltage and radiation values or with numerical approximations-mathematical expressions using experimental data. In direct algorithms, the maximum power point is not obtained by procedures on the contrary to indirect algorithms; the system is forced to operate at MPP. Direct and indirect methods used for determination of maximum power point are examined in the literature. A detailed review of these algorithms is done by Salas et al. [2] and advantages and disadvantages of the algorithms are given. In a study conducted by Berrera et al. [1], seven commonly used MPPT algorithms' MPP tracking performance are compared for two different radiation profiles under standard test conditions. Among the seven generally adopted algorithms, Perturbation and Observe (P&O) algorithm shows the best performance for two different radiation profiles. M. Berrera also states that, Incremental Conductance (IC) algorithm can be a good alternative to P&O algorithm under rapid and continuous irradiance variations. Esram et al. [7], made a comparison of nineteen different MPPT methods according to their cost and performance. The authors state that different algorithms can be suitable for different practice areas. Hohm et al. [8] focus on comparison of three MPPT methods i.e., P&O, IC and Constant Voltage (CV) algorithms, using a PV array simulator. Their performance comparison results show that P&O algorithm is very competitive against other MPP tracking algorithms and can have a better performance in excess of 97%. The study carried out by Hua et al. [9] shows the performance comparison of voltage feedback control, power feedback control and widely used P&O and IC MPPT methods for two different radiation condition. In result of their comparison, among three algorithms IC method shows best performance under two radiation conditions. Reisi et al. [10] compares different MPPT methods with simulation models under Matlab/Simulink.

Their study introduces a classification for MPPT methods based on three categories: hybrid, online and offline methods. As a result of their study, they provide a selection guide of appropriate MPPT methods. Subudhi et al. [11] makes a comprehensive comparison study based on features, like control variables, control strategies, circuitry and approximate costs. Their comparison results offer a useful tool not only for the MPPT users but also the designers and manufacturers of the PV systems. Brito et al. [12] performs the comparison of usual MPPT methods using solar array simulator. They made a comparison between twelve methods with respect to the amount of energy obtained from PV. The authors state that performance differences among the best MPPTs are very slight, and these algorithms must be evaluated according to each situation.

In this part, the case studies of MPPT system, which includes stand-alone and hybrid PV systems, will be briefly reviewed, followed by discussion of the MPPT modeling, design, etc. Several stand-alone and hybrid MPPT application will be presented. Latest developments in MPPT methods will be summarized. Finally some of the present challenges facing the MPPT techniques will be explored. This chapter structured as follows: Sect. 9.2 describes the MPPT techniques and MPPT algorithms modeling; Sect. 9.3 presents the case studies of MPPT techniques, which includes stand-alone and hybrid PV systems; in Sect. 9.4, performance comparison of MPPTs are depicted and at last this part concluded with related discussion.

9.2 Maximum Power Point Tracker

Different MPPT algorithms are used for the determination of MPP. These algorithms are divided into two groups: direct and indirect. The direct methods are; sampling methods, methodology by modulation and other methods. The indirect methods are; curve-fitting, look-up table, open-circuit voltage, short-circuit current and open-circuit voltage of test modules.

9.2.1 Modeling of MPPT Algorithms

This part is presented as a summary of our published conference paper [13]. MPPT algorithms control the PV output to take the PV power to the maximum power point. This control is basically changing of duty-cycle of the dc-dc converter. Duty-cycle changing decision depends on the: PV current in only current photovoltaic (OC) algorithm, short circuit current in short-circuit current (SC) algorithm, PV current and voltage in P&O and IC algorithms. Basic grid-connected PV-battery hybrid system is depicted in Fig. 9.2.

Control part of the dashed diagram (MPPT) in Fig. 9.2 is a MPPT algorithm. Control and Duty part of the MPPT system is depicted as a Matlab/Simulink model in Fig. 9.3.

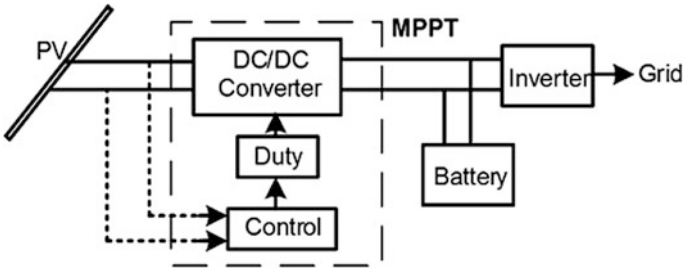

Fig. 9.2 Basic grid-connected PV/battery hybrid system diagram

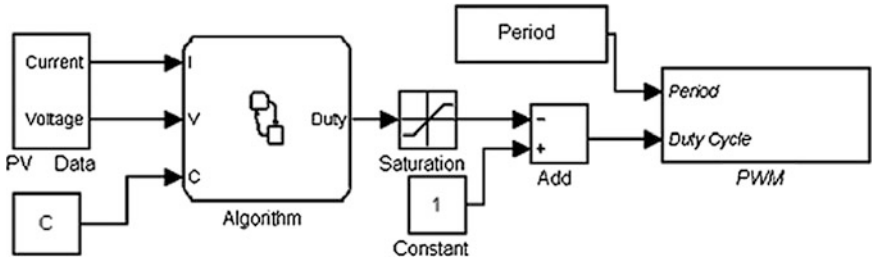

Fig. 9.3 Matlab/Simulink model of the MPPT algorithm

Algorithm blog of the Fig. 9.3 is an actual maximum power point control of the MPPT system. In Fig. 9.3, PV output current, PV output voltage and C (the step-size of the algorithm) input values of algorithm. Duty is an output of the algorithm which is converted to PWM signal.

In this part, Matlab/Stateflow based modeling methodology of four commonly used MPPT algorithms (SC, OC, P&O and IC) are presented. Stateflow is an environment for modeling and simulating combinatorial and sequential decision logic based on state machines and flow charts. Stateflow provides combine tabular and graphical representations, including flow charts, state transition diagrams, state transition tables and truth tables to model how your system reacts to events, time-based conditions, and external input signals. With Stateflow you can design logic for supervisory control, task scheduling, and fault management applications [14].

9.2.1.1 Perturbation and Observe Algorithm

Perturbation and Observe algorithm uses an iterative method to extract maximum power from PV. P&O algorithm measures the power values of PV array and then compares the measured power with prior power to perturb the operation point of PV. If the PV power error is positive, then it changes the duty in same direction. On the other hand, if the PV power error is negative, then it changes the duty in reverse

direction. This duty change continues until PV output power reaches the MPP power level. Figure 9.4 illustrate a basic flowchart and Matlab/Stateflow model of P&O algorithm.

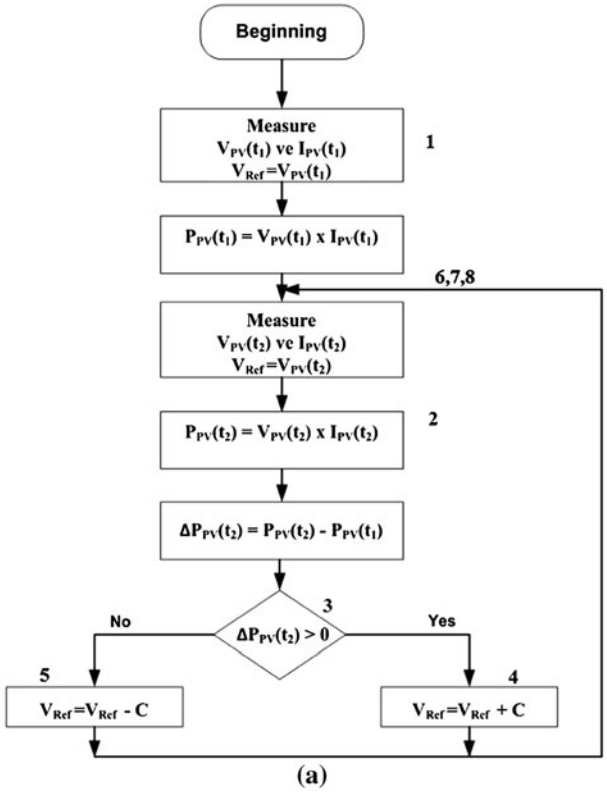

Fig. 9.4 **a** Basic flowchart, **b** Matlab/Stateflow model of P&O algorithm [13]

Table 9.1 Matlab/Stateflow model description of the P&O algorithm

No.	Comment	No.	Comment
1	Beginning	5	Decrease duty
2	Calculate $P_{PV}(t_1)$, $P_{PV}(t_1)$ and ΔP	6	Assign $V_{PV}(t_1)$, $I_{PV}(t_1)$
3	Evaluate ΔP	7	Measure $V_{PV}(t_2)$, $I_{PV}(t_2)$
4	Increase duty	8	Go to 2

Detailed description of the Matlab/Stateflow model in Fig. 9.4 is given in Table 9.1 according to the numbers in the model.

9.2.1.2 Incremental Conductance Algorithm

IC algorithm forced the PV to the MPP based on the observation of conductivity by taking the instantaneous output voltage and output current of PV. Conductivity observation is based on the differentiation of PV power with respect to the PV voltage and setting result to zero. Equations (9.1) and (9.2) give the conductivity observation of the IC method [2].

$$\frac{dP_{PV}}{dV_{PV}} = I_{PV}\frac{dV_{PV}}{dV_{PV}} + V_{PV}\frac{dI_{PV}}{dV_{PV}} = I_{PV} + V_{PV}\frac{dI_{PV}}{dV_{PV}} = 0 \tag{9.1}$$

$$-\frac{I_{PV}}{V_{PV}} = \frac{dI_{PV}}{dV_{PV}} \tag{9.2}$$

In (9.2), the right side of the equation is the incremental conductance and the left side of the equations is the negative conductivity. Figure 9.5 shows the basic flowchart and Matlab/Stateflow model of IC algorithm.

Detailed description of the Matlab/Stateflow model in Fig. 9.5 is given in Table 9.2 according to the numbers in the model.

9.2.1.3 Only Current Photovoltaic Algorithm

In the OC algorithm, the PV is forced to operate at the maximum power point by using only PV current. Equation (9.3) can be obtained from boost type dc-dc converter equation.

$$P_{PV} = V_{PV}I_{PV} = V_o(I_{PV}(1-D)) = P^*_{boost}V_o \tag{9.3}$$

In the OC algorithm, PV current and PV voltage are measured and then PV power is calculated. Then duty-cycle is changed. PV current and PV voltage are measured again and then PV power calculated. PV power compares with prior one.

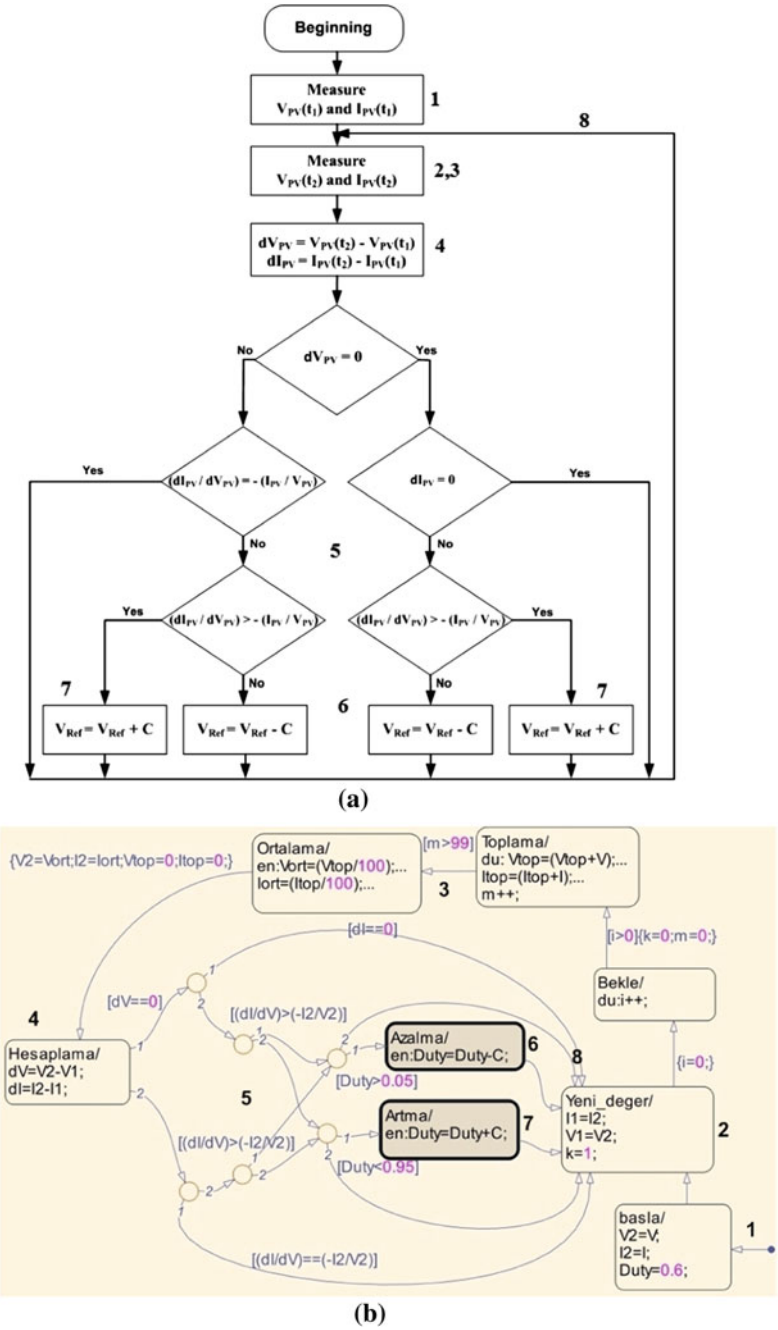

Fig. 9.5 **a** Basic flowchart, **b** Matlab/Stateflow model of IC algorithm [13]

Table 9.2 Matlab/Stateflow model description of the IC algorithm

No.	Comment	No.	Comment
1	Beginning	5	Evaluate conductance
2	Assign $V_{PV}(t_1)$, $I_{PV}(t_1)$	6	Increase duty
3	Measure $V_{PV}(t_2)$, $I_{PV}(t_2)$	7	Decrease duty
4	Calculate dV and dI	8	Go to 2

Table 9.3 Matlab/Stateflow model description of the OC algorithm

No.	Comment	No.	Comment
1	Beginning	5	Evaluate duty
2	Measure $I_{PV}(t_1)$, calculate $P_{PV}(t_1)$	6	Increase/decrease duty
3	Measure $I_{PV}(t_2)$, calculate $P_{PV}(t_2)$	7	Assign $P_{PV}(t_1)$
4	Evaluate $P_{PV}(t_1)$ and $P_{PV}(t_2)$	8	Go to 3

As a result of the comparison, algorithm decides to increase/decrease the duty-cycle. Figure 9.6 shows the basic flowchart and Matlab/Stateflow model of the OC algorithm.

Detailed description of the Matlab/Stateflow model in Fig. 9.6 is given in Table 9.3 according to the numbers in the model.

9.2.1.4 Short Circuit Current Algorithm

SC algorithm depends on the linear relation between maximum power point current and PV short circuit current. The relation is actually a proportional constant (k). The proportional constant mainly depends on the fill factor, solar cells fabrication technology and the environmental conditions [2].

$$k = \frac{I_{MPP}}{I_{SC}} \doteq \text{Constant} < 1 \tag{9.4}$$

SC algorithm flowchart and Matlab/Stateflow model are depicted in Fig. 9.7.

Detailed description of the Matlab/Stateflow model in Fig. 9.7 is given in Table 9.4 according to the numbers in the model.

9.3 Case Studies of the MPPT Algorithms

Many researches in the literature [7–13, 15–21] investigated different MPPT systems. Some of these studies are given below as stand-alone and hybrid application.

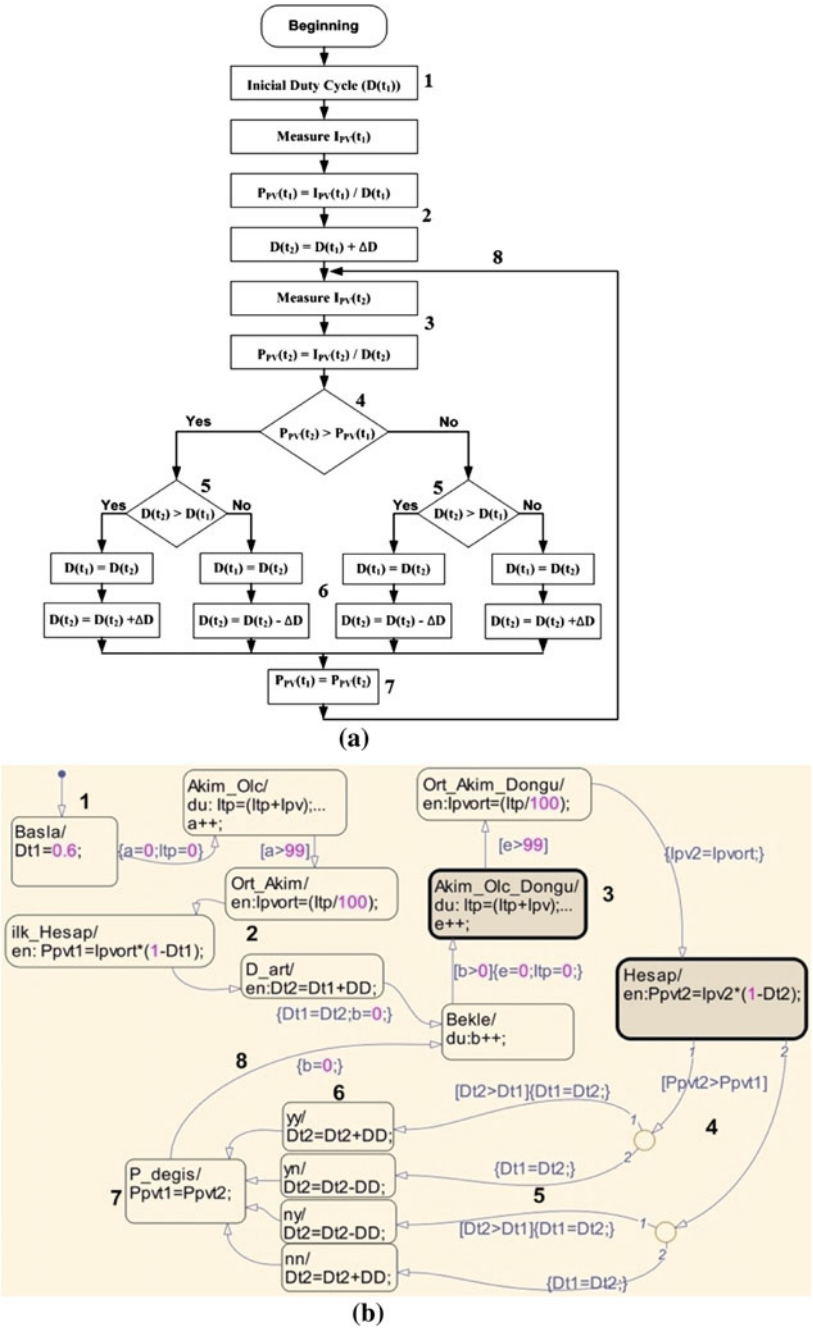

Fig. 9.6 **a** Basic flowchart, **b** Matlab/Stateflow model of OC algorithm [13]

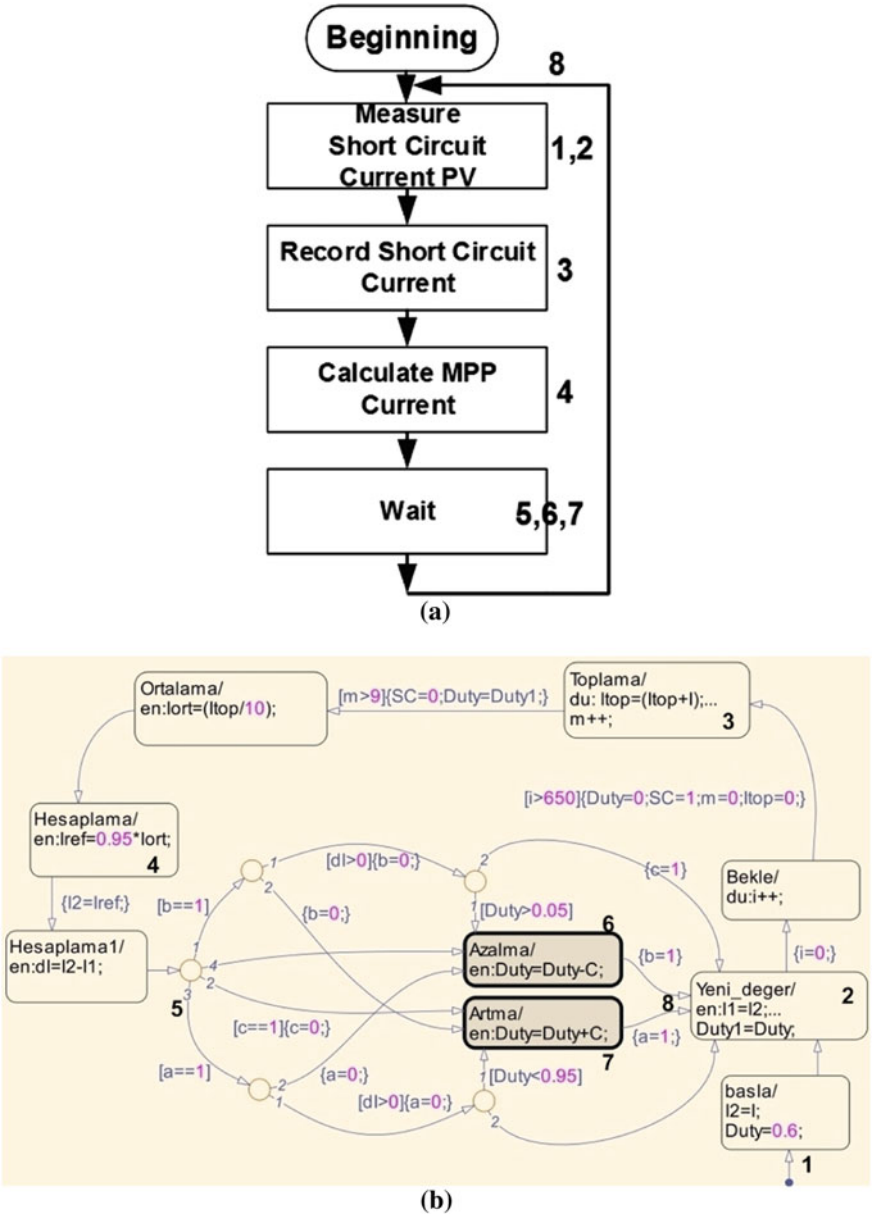

Fig. 9.7 **a** Basic flowchart, **b** Matlab/Stateflow model of SC algorithm [13]

Table 9.4 Matlab/Stateflow model description of the SC algorithm

No.	Comment	No.	Comment
1	Beginning	5	Evaluate I_{MPP}
2	Assign $I_{SC}(t_1)$	6	Decrease duty
3	Measure $I_{SC}(t_2)$	7	Increase duty
4	Calculate I_{MPP}	8	Go to 2

9.3.1 Stand-Alone Applications

Stand-alone applications are given in this part as a summary of our previous published paper [15, 16].

9.3.1.1 Widely-Used MPPT Algorithms Comparison

In this part, unlike the MPPT performance studies which are investigated before, four commonly used MPPT algorithms performances are compared under real ambient conditions. The MPP tracking systems are realized with an experimental setup, which is capable of running four commonly used MPPT algorithms (P&O, IC, OC and SC). As a result under real environmental condition, the performances of the MPPT algorithms are measured and compared [16].

The realized experimental setup is constituted of five main elements: control unit, the dc-dc converters, battery, two identical PV panels and a power analyzer for measuring PV module output values. Figure 9.8 shows the block diagram of the

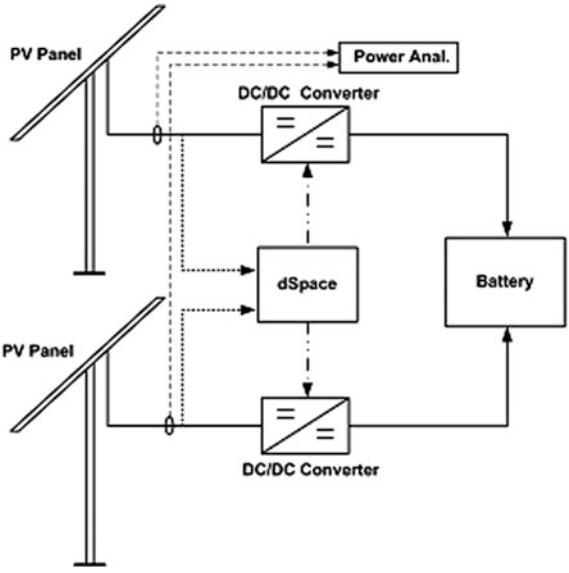

Fig. 9.8 Experimental test system diagram for performance evaluation of MPPT methods [15]

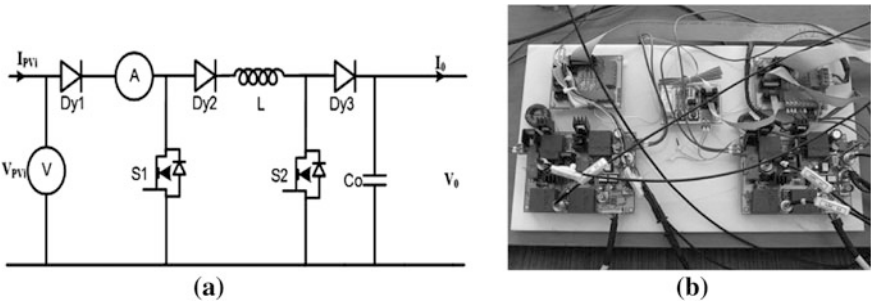

Fig. 9.9 **a** Dc-dc converter circuit, **b** converter power boards [15]

experimental setup. Identical boost type dc-dc converters are connected identical PV panels which are fixed at same position. Dc-dc converters are controlled by the same controller (dSpace). 24 V battery bank is connected to the dc-dc converters' outputs [15].

Step-up type dc-dc converters are employed for the comparison. All of four above mentioned MPPT algorithms can be easily obtained by changing the control algorithm in the control system. Detailed information about dc-dc converter is given in [1]. Converters are operated at 35 kHz frequency. Dc-dc converters control is based on the current and voltage measurements of PV panels which are obtained by hall-effect sensors. Designed power boards and dc-dc converter circuit are depicted in Fig. 9.9. Figure 9.9a also shows that, there is a S1 switch which is necessary for measuring the short circuit current of PV for the SC method.

MPPT algorithms are designed in Matlab/Stateflow Toolbar. Dc-dc converters are controlled by running the algorithms in the dSpace. Herein, algorithm codes are generated in Matlab-Simulink. Basic control scheme of the test bench is shown in Fig. 9.10.

Matlab/Simulink based dSpace control is used for performance comparison of SC, IC, OC and P&O MPPT algorithms. MPP control diagrams for each of algorithm modeled in Matlab/Simulink individually. The algorithm in Fig. 9.10 is a Matlab/Stateflow based designed subsystem of the control unit. The input C (step size of the algorithms) is selected as 0.01 to compare MPPT algorithms under the same conditions.

9.3.1.2 Performance Comparison of MPPT Algorithms for Vehicle Integrated PV Modules

This part presents performance comparison of IC, P&O and OC algorithms examined under real environmental conditions. Performance of algorithms are comparing as a double groups on a special test bench. Potential performance of MPPT algorithms regulating output of solar modules on a vehicle is assessed by controlled moving modules at the special test bench [16].

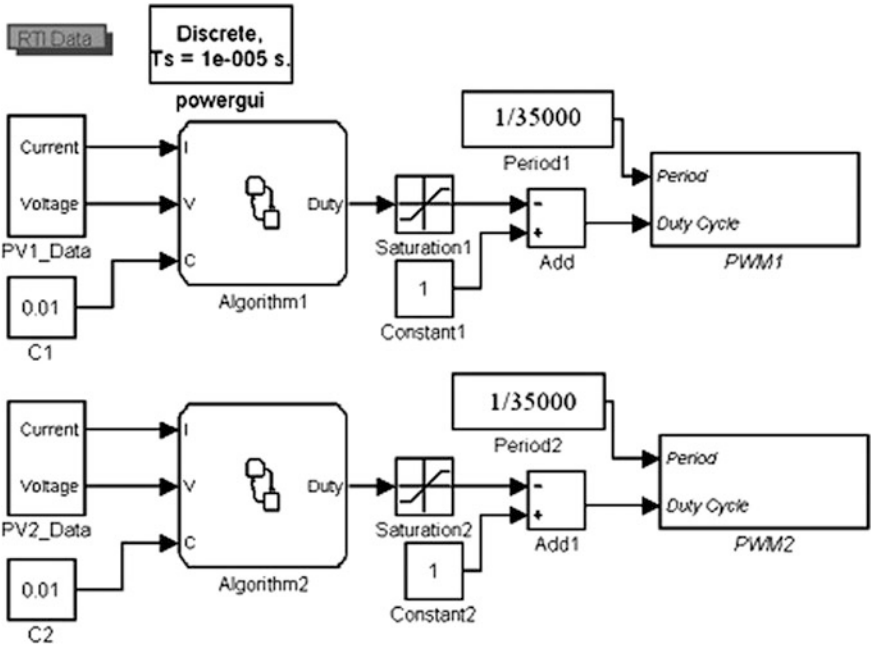

Fig. 9.10 Basic Matlab/Simulink based control scheme of MPPT system [15]

The test bench employed for performance evaluation of MPPT algorithms is constituted from a measurement system (power analyzer) for measuring output power of PV modules, two identical dc-dc converters, two identical PV modules and control unit for employing three MPPT algorithms. The basic block scheme of the test bench is illustrated in Fig. 9.11. PV modules are mounted on test platform to simulate fluctuating irradiance of solar panels on a vehicle in motion. This platform can change both azimuth angle and tilt angle of PV modules. In this study, the platform is moved regarding to a defined motion loop to test realizations of three MPPT algorithms with variation of solar irradiance.

Motion loop of the platform consist of four time intervals and motion ratio of platform is increased at each time interval to simulate fluctuation of solar irradiance with different ratios. This motion loop makes possible to verify responses of MPPT algorithms to the variation of solar irradiance. Consequently, the test platform can simulate instant solar irradiance changes that MPPTs will face for vehicle integrated solar panels. Figure 9.12 shows an example of change in solar radiation of motion loop.

Motion loop of the platform is composed of four time intervals to simulate changing of solar irradiance with higher ratios at each time interval. This effect is simulated by making solar panels move in four different ways with four different motion loops of the platform. Between 0 and 50 s time intervals, only tilt angle slightly changes by time. Between 50 and 100 s time intervals, tilt angle changes are considerably much bigger than first time interval. 100–160 s time intervals are

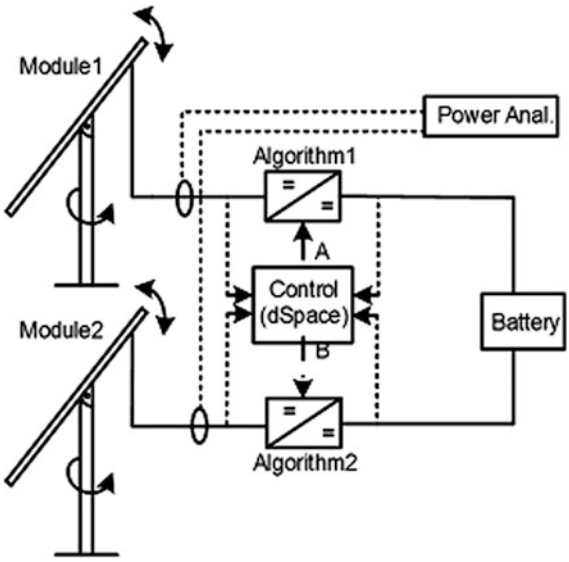

Fig. 9.11 Basic block scheme of the test bench [16]

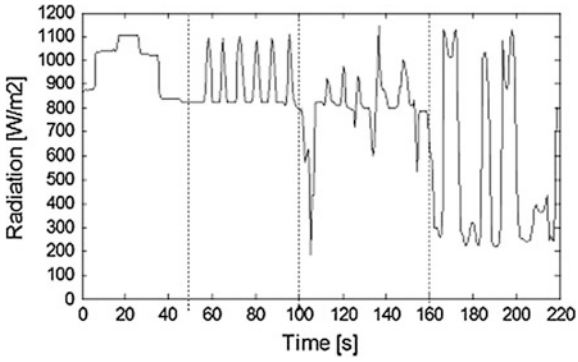

Fig. 9.12 An example of change in solar radiation in motion loop [16]

for changing of both azimuth angle and tilt angle at the same time. Between 160 and 220 s time intervals, while tilt angle of platform is constant, only direction of panels is altered rapidly. As it is understood from each interval, for getting maximum radiation variation, motion of platform is increased from first interval to last interval. Motion loop is designed this way, to measure success of each MPPT algorithms under high variation of solar irradiance which they should deal with for vehicle integrated solar panels.

In the designed test bench, dSPACE is employed as a control unit. This controller manages both control signals of dc-dc converters and defined motion loop simultaneously. Algorithm codes for defined motion loop and dc-dc converters are generated in Matlab/Simulink. Three different control algorithm codes for converters are generated for each MPPT algorithm and implemented as double combinations of three algorithms to compare each other. A sample control diagram, which is modeled in Matlab/Simulink, for one of the comparison is shown in Fig. 9.13.

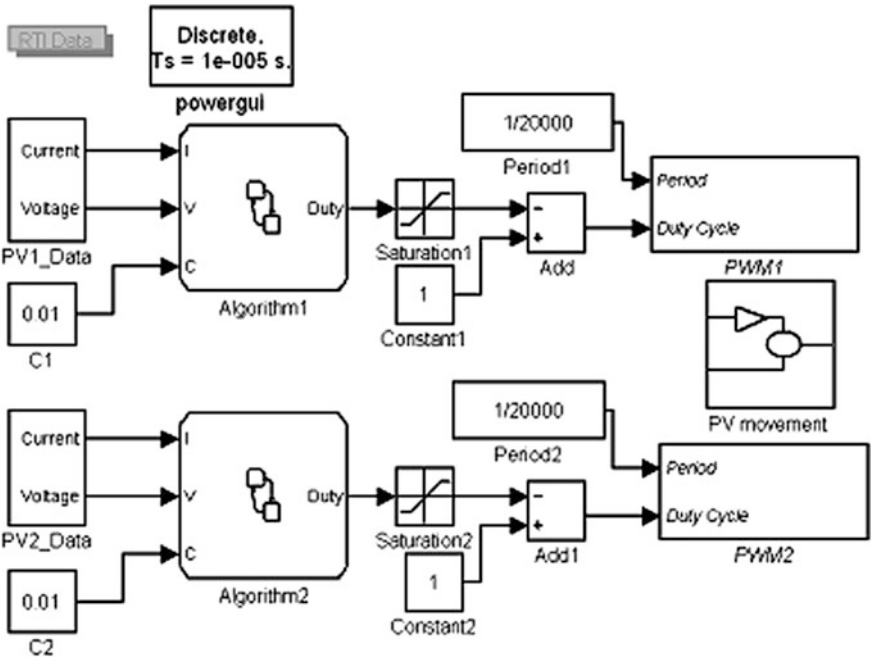

Fig. 9.13 Basic Matlab/Simulink control diagram of the test bench [16]

9.3.2 Hybrid System Application

Hybrid system applications are given in this part as a summary of our previous published paper [17]. In this part, wind-solar-battery hybrid system constructed on the roof of Electrical Engineering Department Building, Yildiz Technical University, Istanbul, Turkey is studied. A wind turbine which is equipped with permanent magnet synchronous generator (PMSG), two PV arrays and battery group are employed as hybrid system equipment in the system. In addition, an inverter, a MPPT controller and a hybrid charge controller are employed as power conditioner unit. A measurement and a data logging system are also exist in the hybrid system. It is planned to realize reliability analysis and wind/solar energy potential of investigated area with measurements.

Hybrid system has eight PV modules. PV modules are divided into two groups. One of the groups (PV1: four modules) is connected to hybrid charge controller with wind turbines. The other PV group (PV2: four modules) is connected to the MPPT charge controller. Hybrid charge controller and MPPT charge controller are connected to 24 V DC bus. Battery group has two series (for reaching the DC bus voltage level) and two parallel elements. Figure 9.14 illustrates the basic block scheme of the wind-solar-battery hybrid system.

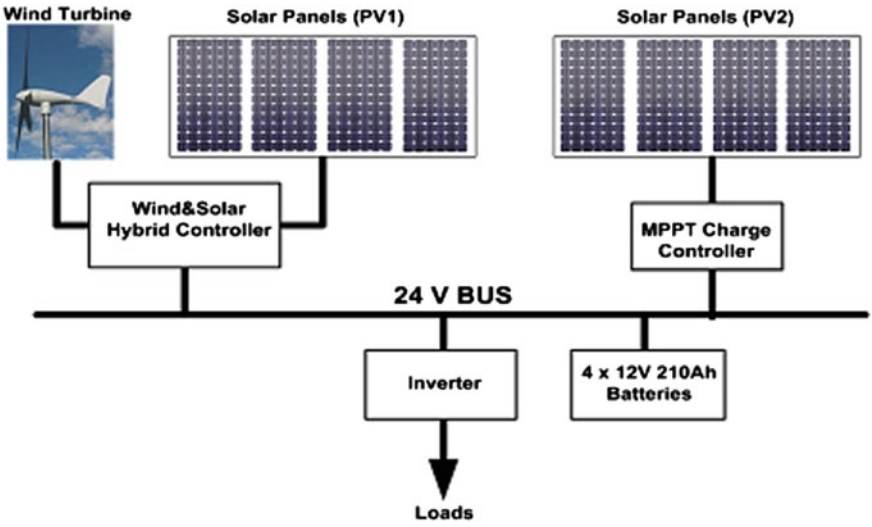

Fig. 9.14 Block diagram of the wind&PV hybrid system [17]

Hybrid charge controller has 1000 W nominal power which is designed for low power wind-solar applications which controls the wind turbine and PV1. Hybrid charge controller adjusts the sources depends on battery voltage level. Moreover, controller also employed for some protection features such as solar wind turbine automatic brake, battery over voltage, cells reverse charging, etc.

MPPT charge controller controls the PV2. MPPT charge controller adjust the PV2 depends on the battery voltage level. Moreover, controller also employed for some protection features such as battery over/deep voltage protection, PV reverse current protection, etc.

The inverter is employed for supplying loads power from DC bus. Inverter has 1000 W nominal power and 3% THD value. Input DC voltage range is various from 21 to 30 V to protect batteries from over charge and deep discharge.

As illustrated in Fig. 9.15, loads are halogen lamps (100 W). Load power is supplied by hybrid system. Three 100 W halogen lamps are connected to system as

Fig. 9.15 Loads of the system

loads. Loads can be switched individual switches to analyze dynamic response of the system.

Measurements, control and the monitoring elements of the hybrid system are depicted in Fig. 9.16.

Fig. 9.16 Measurements, control and monitoring elements of the hybrid system

9.4 Performance Comparison of the MPPTs

9.4.1 Widely-Used MPPT Algorithms Comparison

In this section, the experimental system performances of four algorithms are presented. In this study two identical dc-dc converters are connected to two identical PV panels. These dc-dc converters are controlled by two different MPPT algorithms for a period of 240 s. This comparison process is carried out until all algorithms' comparisons with each other are done. Because two algorithms are compared together on same platform and environmental conditions are same for each PV panel in all comparisons [15].

In order to analyze the performance of four MPP tracking algorithms, algorithms are experimentally compared under medium-high (540–640 W/m^2) radiation level. This comparison process is carried out between 13:35 pm and 14:35 pm time intervals on 26 Dec. 2012. Figure 9.17 shows the wind speed and ambient temperature variation between 13:35 pm and 14:35 pm (1 h) during the comparison process. As it can be seen in Fig. 9.17, while ambient temperature is almost stable, wind speed change between 1–5 m/s. Wind speed decreases the PV temperature which is one of the affecting factor of PV performance. Wind speed variation is neglected in this study due to the PV performance is mainly affected from temperature and radiation. The output power values of PV modules employed by each algorithm are depicted in Fig. 9.18.

Numerical result of these comparisons are given in Table 9.5. The test results show that real environmental conditions, IC algorithm is the most successful MPPT algorithm. However P&O algorithm performance is very close to the IC algorithm. When the P&O algorithm is optimized, the MPP tracking performance of IC and P&O algorithms will be the same. The IC algorithm success based on [15];

- IC algorithm oscillates around the MPP less then P&O algorithm,
- IC algorithm does not diverge from MPP under rapidly changing radiation,
- IC algorithm uses PV current and voltage to track the MPP,
- IC algorithm does not cut the power flow for measuring the PV current/voltage.

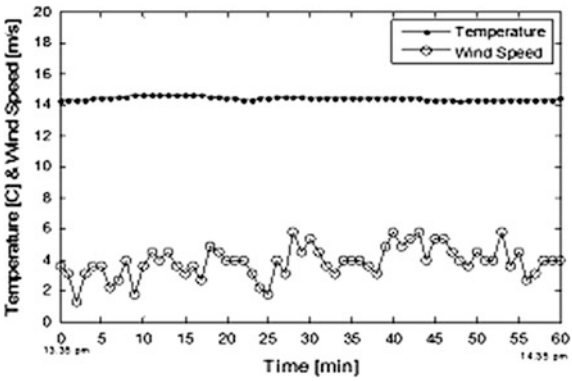

Fig. 9.17 Wind speed and temperature variation during the comparison process [15]

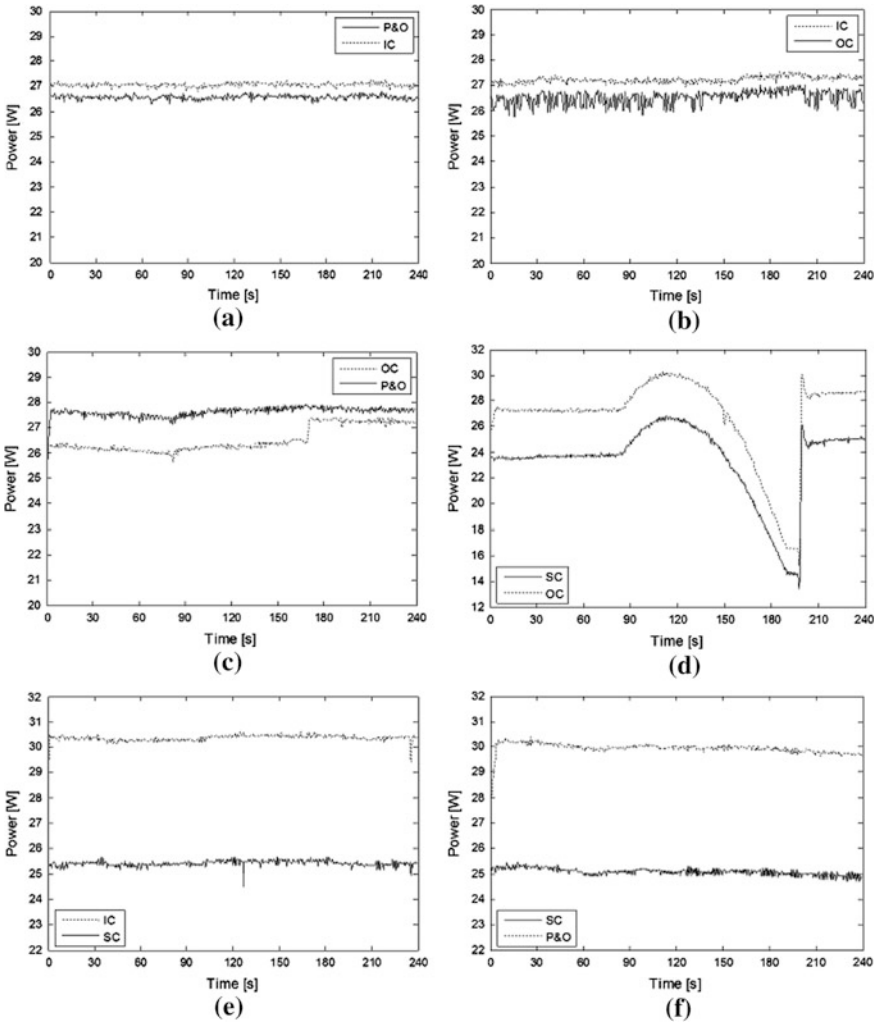

Fig. 9.18 Comparison results of **a** IC and P&O, **b** OC&IC, **c** OC and P&O, **d** SC and OC, **e** IC and SC, **f** SC and P&O algorithms [15]

9.4.2 Vehicle Integrated Solar System

This part presents performance comparison results related to the three MPPT algorithms. Three different algorithms compared as couples between each other and power values are measured. Power output values of each algorithm and the solar radiation variation on PV modules are illustrated in Fig. 9.19.

In Fig. 9.19b, power output result of OC and IC algorithms are depicted. Figure 9.19 confirms natural expectation, that power outputs of both algorithms are

Table 9.5 Numerical results of the comparisons [15]

Comparison	Algorithm	Energy	Delta energy (%)	
			Delta	%
P&O & IC	P&O	6376	IC	1.835
	IC	6493		
OC & IC	OC	6342	IC	2.806
	IC	6520		
OC & P&O	OC	6291	P&O	4.991
	P&O	6605		
SC& IC	SC	6097	IC	19.28
	IC	7273		
SC& P&O	SC	6035	P&O	19.27
	P&O	7198		
SC&OC	SC	5862	OC	14.35
	OC	6703		

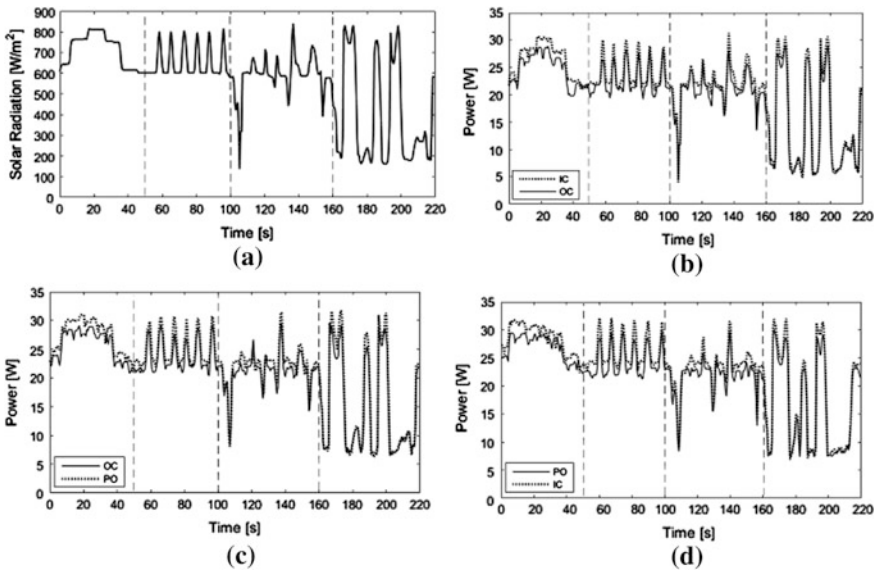

Fig. 9.19 **a** Solar radiation and comparison results of **b** OC and IC, **c** OC and P&O, **d** IC and P&O algorithms [16]

similar with solar radiation. On the other hand, power-time graph in Fig. 9.19b also shows that IC algorithm is more successful at tracking MPP. Total energy data acquired from the power analyzer that are given in Table 9.6 also proves it. Percentage of energy differences in Table 9.7 indicates that efficiency of IC algorithm is 5.536% higher than OC algorithm.

Table 9.6 Numerical results of the four section of motion loop [16]

Comparison	Algorithm	Energy (J)			
		Sect. 1	Sect. 2	Sect. 3	Sect. 4
OC & IC	OC	1234	1132	1233	826
	IC	1309	1190	1306	865
OC & P&O	OC	1290	1173	1273	881
	P&O	1365	1247	1324	925
P&O & IC	P&O	1348	1209	1305	969
	IC	1430	1300	1385	1026

Table 9.7 Energy differences results of the four section of motion loop [16]

Comparison	Delta	Energy differences (Delta energy) (%)				
		Sect. 1	Sect. 2	Sect. 3	Sect. 4	Total
OC & IC	IC	6.077	5.123	5.920	4.721	5.536
OC & P&O	P&O	5.813	6.308	4.006	4.994	5.284
P&O & IC	IC	6.083	7.526	6.130	5.882	6.416

In Fig. 9.19c, power output result of OC and P&O algorithms are depicted. This time P&O algorithm is more successful at tracking MPP. Total energy data in Table 9.6 which is acquired from the power analyzer also verifies this inference. Delta energy data in Table 9.7 reveals that P&O algorithm has 5.284% more total efficiency as compared to OC algorithm.

In Fig. 9.19d, power output result of winners of first and second comparisons are depicted. As depicted in Fig. 9.19d P&O algorithm is less successful than IC algorithm at finding MPP. It is also stated in Tables 9.6 and 9.7 with total energy data and energy differences data respectively. IC algorithm is more successful than P&O algorithm.

The test results show that IC algorithm is the most successful maximum power point tracker algorithm under fast altering solar irradiation. However this performance is not based on success of IC algorithm at radiation fluctuation. This situation is detected from energy differences data in Table 9.7. Although radiation variation values increased at every section, delta energy is not increasing regularly with each section. With presence of these results, it is not possible to show that IC algorithm is more adaptive to variation of irradiance than P&O and OC algorithms. Besides it can be claimed that IC algorithm is the most successful one between three algorithms at tracking MPP also in the case quick variations at irradiation.

9.4.3 Hybrid System

Hybrid system results are given in this part as a summary of our previous published paper [18]. In this study, the effects of two different charge controllers on PV panel performances are investigated as given in Fig. 9.20. The weather conditions and electrical values of the system are recorded simultaneously with a weather station

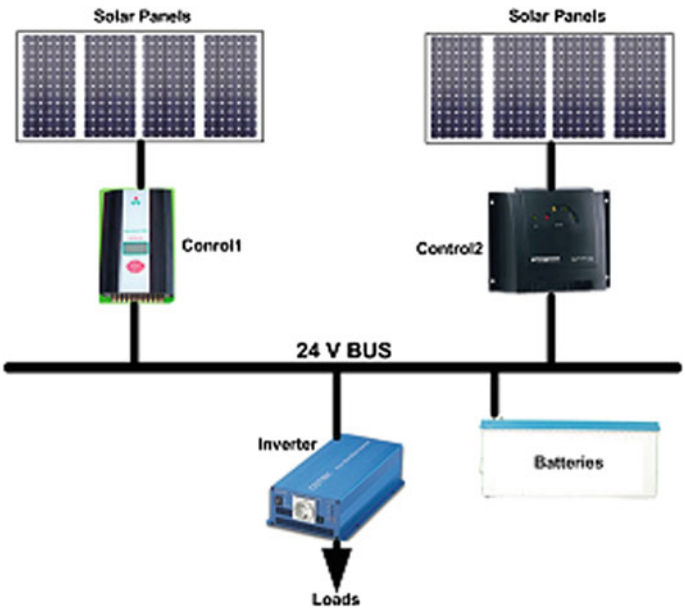

Fig. 9.20 Block diagram of the investigated system [18]

and a data logger. The analyzed data are recorded between 10 Oct. 2013 and 30 Oct. 2013 for 20 days. The variation of solar radiation on the location is shown in Fig. 9.21.

Current and voltage values of PV panels are recorded for duration of a minute. Output voltage and current values of two panels are shown in Fig. 9.22. Vmppt and Imppt define output voltage and current of PV2, V_{hybrid} and I_{hybrid} identify output voltage and current of PV1, and V_{bus} describes DC bus voltage.

DC bus voltage variation is kept in desired limit between 21 and 30 V as clearly seen in Fig. 9.22. The output voltages of both panels drop to 10 V when the solar

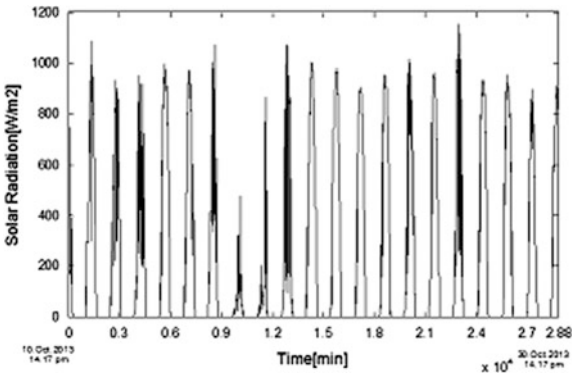

Fig. 9.21 Variation of the solar radiation during the comparison [18]

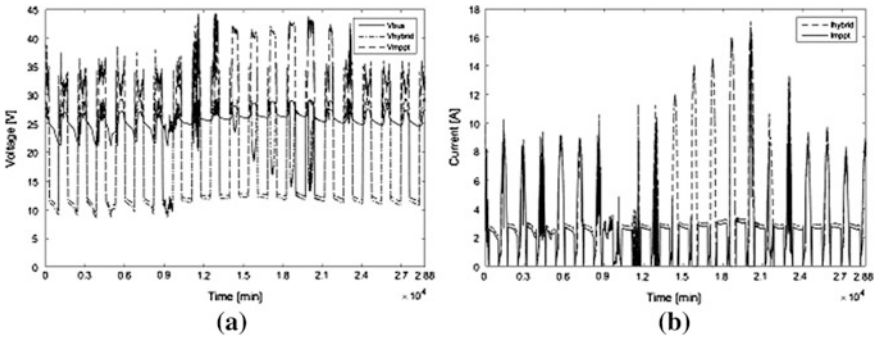

Fig. 9.22 **a** Output voltage, **b** output current of the PV system [18]

radiation is minimum. Output voltage of PV2 increases up to 45 V when the radiation is maximum whereas maximum output voltage of PV1 stays under 30 V.

If the current variations are examined, although PV1 gives higher current than PV2, similar characteristics can be seen in both systems. In the days between 9th and 15th that solar radiation is maximum in, output current of PV2 is minimum since Controller 2 monitors and controls the DC bus voltage to prevent the voltage exceed 27.8 V.

Output power variations of panels are shown in Fig. 9.23. The output power characteristic varies in proportion to solar radiation as seen in Fig. 9.23. Operation characteristic of PV2 panel group controlled by Controller 2 depending on DC bus voltage can be seen clearly in the Fig. 9.23.

Since DC bus voltage reaches to maximum value between 9th and 15th days, Controller 2 restricts the related panel output power. This feature contributes to system stability. In the same time interval, there is no limitation in other panel output power. Although Fig. 9.23 creates perception that the generated power by PV1 is higher than PV2, the total energy obtained from PV1 is 39,826 kWh whereas PV2 is 45,366 kWh in the measurement interval. The energy generated from PV2 is higher by 16.81% from PV1.

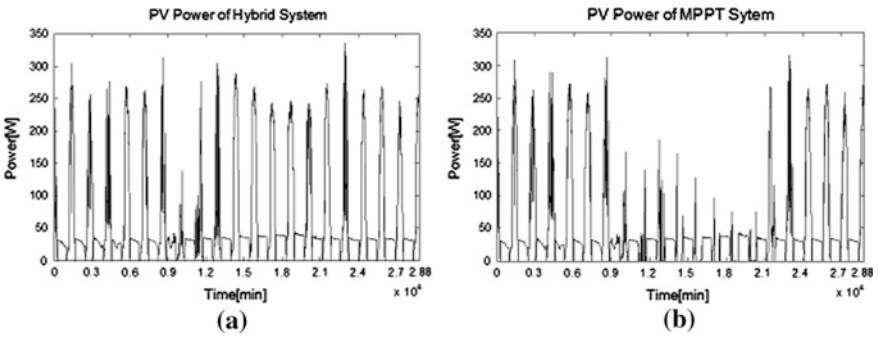

Fig. 9.23 **a** Output power of PVhybrid, **b** output power of the PVmppt [18]

The power difference between two panel groups is caused by Controller 2 that always provides maximum power point operating. While output power of PV1 oscillates in high range, there is stable output power in PV2. It clearly seen from Fig. 9.23a that DC bus voltage is higher than 27.8 V between the days 9th and 14th.

9.5 Conclusion

In this part, the case studies of MPPT system, which includes stand-alone and hybrid PV systems, are briefly reviewed, followed by discussion of the MPPT modeling, design, etc. Several stand-alone and hybrid MPPT application are presented then latest development in MPPT methods will be summarized and finally some of the present challenges facing the MPPT techniques are explored. Case studies and results are presented. Based on the chapter general results, main conclusions are as follows:

- MPPT system has a vital importance for PV applications.
- MPPT system improve the efficiency of PV systems.
- MPPT algorithms performance is affecting environmental conditions.
- The most successful MPPT algorithms among the four commonly used MPP methods is IC.
- The success of IC algorithm is coming from its success in comparison with P&O and OC algorithms at all ambient conditions.
- SC algorithm turned out to be the worst one.
- MPPT controllers have different algorithms and operating principle change the performance of PV modules.
- Controller selection has much importance as panel type, application area and battery size in photovoltaic system design.

References

1. Berrera M, Dolara A, Faranda R, Lova S (2009) Experimental test of seven widely-adopted MPPT algorithms. In: IEEE Bucharest Power Tech Conference, 2009, pp 1–8
2. Salas V, Olias E, Barrado A, Lazaro A (2006) Review of the maximum power point tracking algorithms for stand-alone photovoltaic systems. Sol Energy Mater Sol Cells 90:1555–1578
3. Kalogirou S (2009) Solar energy engineering: processes and systems. Academic Press, New York
4. Markvart T, Castaner L (2003) Practical handbook of photovoltaics fundamentals and applications. Elsevier, UK
5. Renewable Energy Policy Network for the 21st Century (2015) Renewables 2015 global status report. http://www.ren21.net/ren21activities/globalstatusreport.aspx
6. Mutoh N, Ohno M, Inoue T (2006) A method for MPPT control while searching for parameters corresponding to weather conditions for PV generation systems. IEEE Trans Ind Electron 53(4):1055–1065

7. Esram T, Chapman PL (2007) Comparison of photovoltaic array maximum power point techniques. IEEE Trans Energy Convers 22(2):439–449
8. Hohm DP, Ropp ME (2003) Comparative study of maximum power point tracking algorithms. Prog Photovolt Res Appl 11:47–62
9. Hua C, Shen C (1998) Comparative study of peak power tracking techniques for solar storage system. In: IEEE applied power electronics conference and exposition, pp 679–685
10. Reisi AR, Moradi MH, Jamas S (2013) Classification and comparison of maximum power point tracking techniques for photovoltaic system: a review. Renew Sustain Energy Rev 19:433–443
11. Subudhi B, Pradhan RA (2013) Comparative study on maximum power point tracking techniques for photovoltaic power systems. IEEE Trans Sustain Energy 4:89–98
12. Brito MAG, Galotto L, Sampaio LP, Melo GA, Canesin CA (2013) Evaluation of the main MPPT techniques for photovoltaic application. IEEE Trans Ind Electron 60:1157–1167
13. Durusu A, Nakir I, Tanrioven M (2014) Matlab/Stateflow based modeling of MPPT algorithms. Int J Adv Electron Electr Eng 3:117–120
14. MatWorks (2015) Stateflow support documents (Support). http://www.mathworks.com/help/stateflow/index.html
15. Durusu A, Nakir I, Ajder A, Ayaz R, Akca H, Tanrioven M (2014) Performance comparison of widely-used maximum power power point tracker algorithms under real environmental conditions. Adv Electr Comput Eng 14(3):89–94
16. Nakir I, Durusu A, Ugur E, Tanrioven M (2012) Performance assessment of MPPT algorithms for vehicle integrated solar system. In: 2nd IEEE energy conference and exhibition, pp 1034–1038
17. Arikan O, Isen E, Durusu A, Kekezoglu B, Bozkurt A, Erduman A (2013) Introduction to hybrid system-Yildiz Technical University. IEEE Eurocon 2013:1145–1149
18. Arikan O, Kekezoglu B, Durusu A, Isen E, Erduman A, Bozkurt A (2014) Comparison of charge controllers on PV performance: an experimental study. Int J Adv Electron Electr Eng 3:121–125
19. Nakir I, Durusu A, Akca H, Ajder A, Ayaz R, Ugur E, Tanrioven M (2016) A new MPPT algorithm for vehicle integrated solar energy system. J Energy Resour Tech 138 (2):021601-1-9
20. Hsieh GC, Hsieh HI, Tsai CY, Wang CH (2013) Photovoltaic power-increment-aided incremental-conductance MPPT with two-phased tracking. IEEE Trans Power Electron 28:2895–2911
21. Wang F, Wu X, Lee FC, Wang Z, Kong P, Zhuo F (2014) Analysis of unified output MPPT control in subpanel PV converter system. IEEE Trans Power Electron 29(3):1275–1284